The Effects of Dual GLP-1/Glucagon Receptor Agonists with Different Receptor Selectivity in Mouse Models of Obesity and Nonalcoholic Steatohepatitis Ⓢ

Ashref Kayed, Ⓘ Simone Anna Melander, Suheb Khan, Kim Vietz Andreassen, Morten Asser Karsdal, and Kim Henriksen

Nordic Bioscience Biomarkers and Research, Department of Endocrinology, Herlev, Denmark

ABSTRACT

There is an unmet need for nonalcoholic steatohepatitis (NASH) therapeutics, considering the increase in global obesity. Dual GLP-1/glucagon (GCG) receptor agonists have shown beneficial effects in circumventing the pathophysiology linked to NASH. However, dual GLP-1/GCG receptor agonists as a treatment of metabolic diseases need delicate optimization to maximize metabolism effects. The impacts of increased relative GLP-1/GCG receptor activity in NASH settings must be addressed to unleash the full potential. In this study, we investigated the potential of OXM-104 and OXM-101, two dual GLP-1/GCG receptor agonists with different receptor selectivity in the setting of NASH, to establish the relative receptor activities leading to the best metabolic outcome efficacies to reduce the gap between surgery and pharmacological interventions. We developed dual GLP-1/GCG receptor agonists with selective agonism. Despite the improved metabolic effects of OXM-101, we explored a hyperglycemic risk attached to increased relative GCG receptor agonism. Thirty-eight days of treatment with a dual GLP-1/GCG receptor agonist, OXM-104, with increased GLP-1 receptor agonism in obese NASH mice was found to ameliorate the development of NASH by lowering body weight, improving liver and lipid profiles, reducing the levels of the fibrosis marker PRO-C4, and improving glucose control. Similarly, dual GLP-1/GCG receptor agonist OXM-101 with increased relative GCG receptor agonism ameliorated NASH by eliciting dramatic body weight reductions to OXM-104, reflected in the improvement of liver and lipid enzymes and reduced PRO-C4 levels. Optimizing dual GLP-1/GCG agonists with increased relative GCG receptor agonism can provide the setting for future agonists to treat obesity, type 2 diabetes, and NASH without having a hyperglycemic risk.

SIGNIFICANT STATEMENT

There is an unmet need for nonalcoholic steatohepatitis (NASH) therapeutics, considering the increase in global obesity. Dual GLP-1/glucagon (GCG) receptor agonists have shown beneficial effects in circumventing the pathophysiology linked to NASH. Therefore, this study has examined OXM-104 and OXM-101, two dual GLP-1/GCG receptor agonists in the setting of NASH, to establish the relative receptor activities leading to the best metabolic outcome efficacies to reduce the gap between surgery and pharmacological interventions.

Introduction

The prevalence of overweight (BMI ≥25) and obesity (BMI ≥ 30) has been increasing for the past 50 years, resulting in increased incidences of metabolic syndrome, a cluster of metabolic abnormalities covering insulin resistance, dyslipidemia, nonalcoholic fatty liver disease (NAFLD), hypertension, and central obesity (Younossi et al., 2018; World Health Organization, Diabetes, 2020, https://www.who.int/news-room/fact-sheets/detail/diabetes; World Health Organization, Obesity and overweight, 2020, https://www.who.int/news-room/fact-sheets/detail/obesity-and-overweight). In recent years, monoreceptor-acting incretins such as glucagon-like peptide 1 (GLP-1) receptor agonists have been extensively investigated as antiobesogenic and antidiabetic therapeutics. The GLP-1 receptor agonists induce postprandial insulin secretion and decrease glucagon secretion while increasing satiety, slowing gastric motility, and enhancing β-cell health (Holst, 2007). Recently, GLP-1 receptor agonists have emerged as a potential treatment of NAFLD's progressive form, known as nonalcoholic steatohepatitis (NASH), due to beneficial effects on metabolism leading to NASH resolution (Armstrong et al., 2016; Newsome et al., 2021).

The evolution has previously inspired the development of drugs targeting diseases such as arthritis, osteoporosis, obesity, and type 2 diabetes (Sexton et al., 1999; Henriksen et al.,

ABBREVIATIONS: ALP, alkaline phosphatase; ALT, alanine transaminase; AST, aspartate transaminase; Chol, cholesterol; FBG, fasting blood glucose; GCG, glucagon; GLP-1, glucagon-like peptide 1; HDL, high-density lipoprotein; LDL, low-density lipoprotein; NAFLD, nonalcoholic fatty liver disease; NASH, nonalcoholic steatohepatitis; OGTT, oral glucose tolerance test; PF, pair-fed; QW.III, every third day; tAUC, total area under the curve; TG, triglyceride.

2010; Gydesen et al., 2016; Katri et al., 2019). The idea of using evolution as an inspirational source has previously shown that paddlefish glucagon (GCG) is structurally similar to the GLP-1 receptor agonist exendin-4 and improves glucose control (Graham et al., 2018). Moreover, the European dogfish GCG exhibited promising insulinotropic effects in vitro and in mice (O'Harte et al., 2016). GCG is a peptide hormone known to increase glucose through gluconeogenesis and glycogenolysis. Furthermore, GCG drives body weight reductions through its effects on satiety and energy expenditure (Müller et al., 2017).

Oxyntomodulin, a peptide hormone released from the gut with dual GLP-1 and GCG receptor activity, has been an inspiration source for therapeutics targeting obesity, type 2 diabetes, and NASH(Henderson et al., 2016; Boland et al., 2020). Dual GLP-1/GCG receptor agonists have been shown to induce more significant body weight–lowering effects than selective GLP-1 receptor agonists, thus highlighting the potential of dual GLP-1/GCG receptor agonism (Elvert et al., 2018). Moreover, combinational treatments enhancing metabolism have attracted more attention in recent years due to their beneficial effects on lowering body weight.

In this context, the direct effects of dual GLP-1/GCG agonists on GCG receptor activation in the liver have shown great promise as a potential treatment of NASH (Boland et al., 2020). The classic view of GCG as the opposing insulin hormone has limited its use as a therapeutic agent. Previously, relative receptor activity was crucial as it may deteriorate glucose control (Day et al., 2012). Hence, a thorough understanding of relative GCG receptor activity to relative GLP-1 receptor activity is required to gain knowledge about peptide designs to treat obesity, type 2 diabetes, and, especially, NASH.

Therefore, we developed two long-acting GLP-1/GCG receptor agonists, OXM-104 and OXM-101. OXM-104 was designed with an increased relative GLP-1 receptor activity, whereas OXM-101 was designed with an increased relative GCG receptor activity. These ligands were examined in obese mice and obese NASH mice to determine the effects on body weight reductions, glucose control, liver and lipid profiles, and NASH resolution.

Materials and Methods

Peptide Therapy. Synthetic oxyntomodulin mimetics (Synpeptide, Shanghai, China) were dissolved in phosphate-buffered saline at a stock concentration of 1 mM. For in vivo testing, stocks were further diluted to the desired concentration in 0.9% NaCl.

In Vitro Peptide Screening. The dual GLP-1/GCG receptor agonists' potencies at the GCG receptor and GLP-1 receptor were determined using the PathHunter β-Arrestin G protein-coupled receptor assay. Cell lines heterologously expressing the GLP-1 receptor (CHO-K1 GLP1R, DiscoveRx; cat. no.: 93-0300C2) and GCG receptor (CHO-K1 GCGR, DiscoveRx; cat. no.: 93-0241C2) were used. All experiments were conducted using 2500 cells per well in 10-μL cell type in Gibco's Ham's F-12 Nutrient Mix (cat. no. 21765-037) from Invitrogen, with the addition of fetal bovine serum (10% cultivation and 0.1% during experimentation), 400 μg/mL hygromycin B, 800 μg/mL Geneticin, and penicillin/streptomycin 1 U. To quantify the G protein-coupled receptor mediated β-arrestin recruitment, the PathHunter Detection Kit (93-0001, DiscoverX) was used, and the assay was performed according to the manufacturer's instructions. In vitro screening of peptides was performed with ligand concentrations starting from 20 μM.

Animal Experiments. Animal studies were conducted according to the institutional license issued to Nordic Bioscience (2020-15-0201-00614) by the Animal Experiment Inspectorate under the Ministry of Environment and Food of Denmark and were performed under guidelines from the Animal Welfare Division of the Danish Ministry of Justice. Twelve-week-old female C57BL/6JOlaHsd mice (Envigo, Netherlands) and 5–7-week-old male MSNASH/PcoJ (The Jackson Laboratory) were quad-wise housed under controlled temperature (21 to 22°C) on a standard 12-hour light/dark cycle (lights on 1900) with ad libitum access to water and food in a standard Type III H cage. C57BL/6JOlaHsd were fed a standard high-fat diet (D12495, Research Diets Inc), and MSNASH/PcoJ mice were fed a Gubra Amylin Nash diet consisting of 40% kcal fat (palm oil), 20% kcal fructose, and 2% cholesterol (D09100310, Research Diets Inc). All animals were allowed ad libitum access to food and water for 8–16 weeks before study initiation and for treatment groups throughout the rest of the study period. Pair-feeding groups had restricted access to food throughout the treatment period, where the amount of food provided matched that consumed by the matched treatment group.

Acute Potency Test. According to body weight, 40 female C57BL/6JOlaHsd mice (~60 weeks old) were allocated into treatment groups (n = 8/group). Mice received a single subcutaneous administration of vehicle (0.9% NaCl), OXM-104 or OXM-101 at 12.5 and 25 nmol/kg. Body weight and food intake were monitored every 24 hours for 96 hours.

Chronic Study in High-Fat Diet (Obese) Mice. According to body weight, 96 female C57BL/6JOlaHsd mice (~26 weeks old) were allocated into treatment groups (n = 8–16 mice/group). For 35 days, mice received subcutaneous administration of either vehicle (0.9% NaCl) or OXM-101 at 12.5–25 nmol/kg or OXM-104 25 nmol/kg every third day (QW.III). Pair-feeding groups to OXM-104 and OXM-101 were introduced as a surrogate marker for energy expenditure. The pair-fed (PF) groups received administrations of 0.9% NaCl (QW.III). Body weight and food intake were monitored every 24 hours, and 5 weeks into the study, an oral glucose tolerance test (OGTT) was performed. Animals were euthanized, followed by exsanguination and dissection, at study termination. Inguinal and perirenal adipose tissue and liver were surgically removed and weighed.

A Chronic Intervention Study in Obese/NASH Mice. Twenty-eight male MSNASH/PcoJ (FATZO ~16–18 weeks old) were allocated into treatment groups according to body weight (n = 8–10 mice/group). For 38 days, mice received subcutaneous administrations of either vehicle (0.9% NaCl), OXM-101 30 nmol/kg, or OXM-104 30 nmol/kg (QW.III). All mice initiated a four-step dose escalation regimen. At study start, all groups received 7.5 nmol/kg; on day 7, all groups escalated to 15 nmol/kg; on day 13, all groups escalated to 22.5 nmol/kg; and on day 19, all groups escalated to full dose. Body weight and food intake were monitored every 24 hours, and 6 weeks into the study, an OGTT was performed. Animals were euthanized, followed by exsanguination and dissection, at study termination. Inguinal and perirenal adipose tissue and liver were surgically removed and weighed. Five-hour fasting blood glucose (FBG) was measured 1 week before the study started, again at week 5, and at termination (week 8).

OGTT. Overnight-fasted mice received glucose by oral gavage (5 g/kg in C57BL/6JOlaHsd and 2 g/kg in MSNASH/PcoJ). Blood glucose was measured by the Accu-Check Avia monitoring system (Roche Diagnostics, Rotkreuz, Switzerland) at 0, 15, 30, 60, 120, and 180 minutes using a drop of tail blood.

Biochemical Analysis. Blood samples were collected in EDTA tubes and centrifuged at 5000 rpm for 10 minutes at 4°C. Plasma insulin levels (Mercodia mouse Insulin ELISA, Mercodia AB, Uppsala, Sweden) were analyzed according to manufacturer instructions. Alanine transaminase(ALT), aspartate transaminase (AST), alkaline phosphatase (ALP), triglyceride (TG), low-density lipoprotein (LDL), high-density lipoprotein (HDL), and cholesterol (chol) levels were measured in house (ADVIA 1800, Siemens Healthineer, Germany). Basement membrane type IV collagen, PRO-C4 (Nordic Bioscience A/S, Herlev) was assessed by a validated competitive ELISA (Leeming et al., 2012). A streptavidin-coated 96-well plate, with the appropriate biotinylated peptide, was incubated for 30 minutes in the dark at 20°C while shaking (300 rpm) and was subsequently washed in washing buffer. Twenty microliters of controls and samples was added to

the wells together with 100 μL horseradish peroxidase–conjugated monoclonal antibody. The plate was incubated for 1 hour at 20°C in the dark while shaking and was washed in washing buffer. One-hundred microliters of substrate solution were added to each well for 15 minutes and left in the dark while shaking, following 100 μL of stopping solution. Plates were measured at 450 nm with 650 nm as reference.

Histologic Analysis. Liver tissue fixed in 10% neutral-buffered formalin for 48 hours was paraffin embedded using a Sakura Tissue Tek VIP 5 Jr. Tissue Processor and cut on an HM 360 microtome in 5-μm-thick slides. The staining procedure started with 1 hour of melting paraffin, followed by deparaffinization and rehydration. Stained slides were analyzed with an Olympus BX60 microscope attached to an Olympus DP71 camera at 2×–20× magnification.

Sirius Red staining: Liver slides were incubated in Weigert's Hematoxylin for 8 minutes. Slides were next placed in running tap water for 5 minutes and stained with a 0.1% Sirius Red (36554, Sigma Aldrich) solution dissolved in aqueous saturated picric acid for 1 hour, followed by dehydration and mounting with a toluene-based glue.

Hematoxylin and eosin staining: Following rehydration, liver slides were incubated in Mayer's hematoxylin for 5 minutes. Slides were placed in running tap water for 5 minutes, counterstained with eosin for 4 minutes, and washed in running tap water for 5 minutes. Slides were next dehydrated and mounted with a toluene-based glue.

A modified NAFLD activity score composed of a steatosis (0–3), microvesicular steatosis (0 to 1), inflammation (0 to 1), and fibrosis stage (0–4) was used to evaluate the effects on NASH. We completed scoring of liver health under blinded conditions (one slide per animal at three depths 150 μm apart). Slides were examined using an Olympus BX60 microscope attached with an Olympus DP71 camera at 4×–20× magnification. Specific magnification for each picture is stated in the respective figures.

Statistical Analysis. Data were statistically analyzed by one-way ANOVA and Bonferroni's multiple comparison post hoc test or by Kruskal-Wallis test comparison and Dunn's post hoc test. All analyses and graphical presentations were performed using GraphPad Prism 9 (GraphPad Software, San Diego, CA). Results are expressed as mean ± S.E.M. unless otherwise stated. $P < 0.05$ was considered statistically significant, shown with one symbol; $P < 0.01$ is shown with two symbols; and $P < 0.001$ is shown with three symbols. *Significant from the vehicle; #significant from pair-fed groups or comparison between agonists with increased relative activity.

Results

In Vitro Characterization and Acute in Vivo Testing of OXM-104 and OXM-101. The sequences and modifications of OXM-104 and OXM-101 are shown in Table 1. Potency (EC50) for OXM-104 was 47.1 ± 16.4 nM at the GLP-1 receptor and 2.1 ± 1.1 μM at the GCG receptor, whereas OXM-101 potency at the GLP-1 and GCG receptor was 22.3 ± 8.4 nM and 0.2 ± 0.2 μM, respectively. For OXM-104 and OXM-101, approximately equivalent potencies were observed at the GLP-1 receptor, whereas OXM-101 showed a 9.5-fold borderline-significant ($P = 0.07$) potency increase at the GCG receptor compared with OXM-104. These findings indicated that OXM-101 had a strong GCG receptor selectivity, whereas OXM-104 favored the GLP-1 receptor. Moreover, the acute in vivo effects of OXM-104 and OXM-101 on body weight reductions and food intake were examined in obese mice to establish the applicable dose range for chronic tests applied in this study. During the acute test, the lowest dose of OXM-104 and OXM-101 reduced body weight by 5.0% ± 1.0% and 4.2% ± 0.4% compared with vehicle (Supplemental Fig. 1A). Furthermore, the highest dose of OXM-104 and OXM-101 led

TABLE 1
Sequence overview of OXM-104 and OXM-101 and in vitro potency at the GLP-1 and GCG receptor
β-Arrestin recruitment assays were used to establish EC50 (nanomolar) values from n ≥ 3 independent experiments, which formed the basis for GLP-1/GCG receptor ratio calculations. A two-tailed unpaired *t* test analyzed potencies. Data are mean ± S.E.M.

Peptide Sequences of Selective GLP-1/GCG Receptor Agonists
OXM-104: - H X Q G T F T S D Y S K Y L D K(Ac) R R A R D F V Q W L M N T K R N G Q Q G Q -NH2
OXM-101: - H X Q G T F T S D Y S K Y L D K(Ac) R R A R D F V Q W L M N T -NH2X: Aminoisobutyric acid
K(Ac): γ-Glu-γ-Glu-C20 diacid conjugated to lysine

	GLP-1 Receptor	GCG Receptor	GCG Receptor/GLP-1 Receptor Ratio
		OXM-104	
EC50	47.1	2057.9	43.7
S.E.M.	16.4	1092.4	
		OXM-101	
EC50	22.3	216.1 $P = 0.07$	9.7
S.E.M.	8.4	150.8	

to a 7.4% ± 0.9% and 8.3% ± 0.7% reduction in body weight compared with vehicle (Supplemental Fig. 1A). Body weight reductions were reflected in an immediate suppression of food intake, which lasted for 24 hours, as seen in the mice receiving low doses of OXM-104 and OXM-101. In mice treated with the highest dose of OXM-104 and OXM-101, food suppression lasted for 48 hours, after which it normalized (Supplemental Fig. 1B).

Head-to-Head Comparison of OXM-104 and OXM-101 on Caloric Intake, Body Weight, and Energy Expenditure. OXM-104 and OXM-101 were synthesized and tested in obese mice to investigate the effects of different receptor selectivities. OXM-104 and OXM-101 significantly lowered body weight compared with vehicle (Fig. 1, A and C). A 17.1% ± 4.2% and 32.0% ± 2.8% body weight loss was observed in mice on OXM-104 and OXM-101 treatment. The absolute body weight in OXM-104 and OXM-101 mice was 33.7 ± 2.2 g and 24.8 ± 0.7 g, respectively, at the end of the study (Fig. 1B). OXM-101 drove dramatic reductions in body weight, which, for ethical considerations, required a dose halving of OXM-101 from day 13 (Fig. 1A). Pair-feeding groups were included to investigate the effects of selective agonism beyond energy intake (Fig. 1A). Matching of food intake resulted in evident body weight reductions compared with vehicle mice (Fig. 1, A and C). PF-OXM-104 and PF-OXM-101 mice significantly ($P < 0.05$) reduced body weight by 21.4% ± 3.2% and 24.8% ± 6.7% compared with vehicle mice (Fig. 1C). Effects on body weight reductions beyond energy intake were examined by comparing OXM-104 and OXM-101 to their corresponding pair-fed treatment groups. By comparing OXM-104 to PF-OXM-104 and OXM-101 to PF-OXM-101, a tendency for increased reduction in body weight was observed in both OXM-104 and OXM-101 (Fig. 1C). A further increased body weight reduction of 7.9% ± 4.7% was observed in OXM-104 mice compared with PF-OXM-104, whereas OXM-101 treatment showed a borderline-significant ($P = 0.06$) 23.1% ± 3.2% reduction in body weight compared with PF-OXM-101 (Fig. 1C). Reductions in body weight were reflected in the suppression of caloric intake compared with vehicle (Fig. 1D). Caloric intake was reduced by 22.7% and 37.4% in OXM-104 and OXM-101 mice compared with vehicle. In line with the apparent reductions in
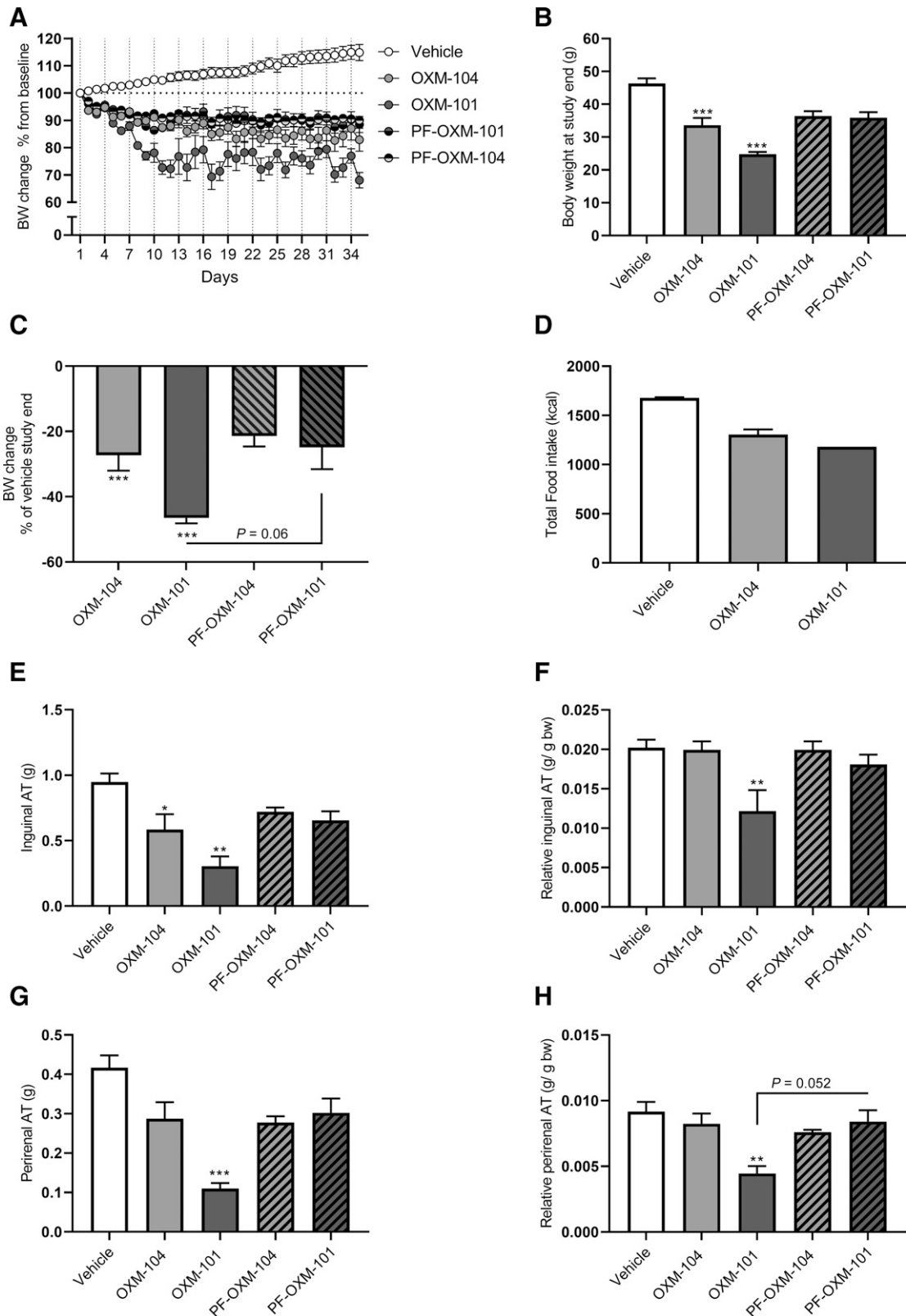
Fig. 1. Chronic effects of OXM-104 and OXM-101 on body weight (bw), food intake, and adipose tissue weights in obese mice after 35 days with vehicle ($n = 16$), OXM-104 ($n = 8$), OXM-101 ($n = 4$), PF-OXM-104 ($n = 8$), and PF-OXM-101 ($n = 4$). (A) Body weight change (percentage of initial body weight) throughout the study. (B) Endpoint body weights (g). (C) Column graphs illustrating study-end body weight changes (percentage of vehicle). (D) Accumulated caloric intake expressed in kcal/4 mice. (E) Absolute weight of inguinal adipose tissue. (F) Relative weight of inguinal adipose tissue. (G) Absolute weight of perirenal adipose tissue. (H) Relative weight of perirenal adipose tissue. Dotted lines shown in (A) designate dosing days. Statistical analysis between groups was evaluated by one-way ANOVA and Bonferroni's multiple comparison post hoc test, except for (E), (G), and (H), which were analyzed by a Kruskal-Wallis test and Dunn's multiple comparison post hoc test. $*P < 0.05$; $**P < 0.01$; $***P < 0.001$ compared with vehicle mice. $\#P < 0.05$ when compared with OXM-101. Data are mean ± S.E.M.

body weight, treatment with OXM-104 and OXM-101 significantly reduced the absolute weights of inguinal adipose tissue in OXM-104 and OXM-101 mice compared with vehicle (Fig. 1E). Absolute weights of perirenal adipose tissue in OXM-104 mice showed a tendency for reduction, whereas a significant decrease was found in OXM-101 mice compared with vehicle (Fig. 1G). Inguinal and perirenal adipose tissue weights relative to body weight for OXM-104 mice were almost equal to relative inguinal and perirenal vehicle weights. In contrast, relative inguinal and perirenal adipose tissue was significantly reduced compared with vehicle. In addition, relative perirenal adipose tissue showed a borderline-significant ($P = 0.05$) reduction compared with PF-OXM-101 (Fig. 1, F and H).

Repeated Administration of OXM-101 Followed by an OGTT-Impaired Glucose Tolerance in Obese Mice. The day before the study ended, an OGTT was conducted to investigate the effects of glucose tolerance and glucose control (Fig. 2, B and C). FBG levels at OGTT baseline indicated a significant treatment effect of OXM-104 and a slight tendency for a treatment effect of OXM-101 compared with vehicle (Fig. 2A). OXM-104 and OXM-101 mice had a significantly lower baseline FBG than their respective pair-fed groups (Fig. 2A). The total glucose area under the curve (tAUC), an index of glucose excursion during an OGTT, was significantly decreased by OXM-104 (Fig. 2D). The tAUC decreased by 24.5% ± 1.9% and 21.7% ± 5.3% compared with vehicle and PF-OXM-104, respectively (Fig. 2D). In contrast, OXM-101 mice increased the tAUC by 7.6% ± 5.3% and 8.2% ± 7.6% compared with vehicle and PF-OXM-101, respectively (Fig. 2D). Incremental areas under the curve showed a tendency for improved glucose tolerance in OXM-104 mice, whereas OXM-101 mice showed a tendency for glucose intolerance compared with vehicle (Fig. 2E).

Effects of Selective GLP-1/GCG Receptor Agonists on Body Weight Reductions and Plasma Lipid Profiles in Obese NASH Mice. Treatment with OXM-104 and OXM-101 in obese NASH mice significantly lowered body weight compared with vehicle (Fig. 3, A–C). OXM-104 mice reduced body weight by 10.5% ± 4.2% from baseline, whereas OXM-101 mice reduced body weight by 46.3% ± 0.9%. Furthermore, tAUC for body weight changes was reduced by OXM-104 and OXM-101 compared with vehicle (Fig. 3C). tAUCs in the OXM-104 and OXM-101 groups reduced by 7.7% ± 0.6% and 21.6% ± 0.6%, respectively. Interestingly, body weight reductions were not driven by caloric intake reductions among the treatment groups (Fig. 3C). Absolute weights of inguinal, epididymal, and perirenal adipose tissue were measured at study end (Fig. 3, E–G). In line with the apparent reductions in body weight, OXM-104 and OXM-101 significantly reduced inguinal, epididymal, and perirenal adipose tissue compared with vehicle (Fig. 3, E–G). Furthermore, OXM-101 significantly reduced inguinal, epididymal, and perirenal adipose tissue compared with OXM-104. Adipose tissue weights of inguinal, epididymal, and perirenal depots relative to body weight are presented in Supplemental Fig. 2. Interestingly, changes in plasma chol levels from baseline were significantly reduced in OXM-104 and OXM-101 compared with vehicle. Plasma chol levels in OXM-104 and OXM-101 mice were reduced by −0.3 ± 0.3 mmol/L and −3.5 ± 0.2 mmol/L, respectively (Table 2). In conjunction, changes in plasma LDL and HDL levels showed opposing patterns (Table 2). OXM-104 and OXM-101 mice significantly reduced plasma LDL levels compared with vehicle (Table 2).

Interestingly, OXM-104 mice showed a 0.1 ± 0.1 mmol/L modest increase in plasma LDL levels from the baseline, whereas OXM-101 decreased plasma LDL levels by −0.2 ± 0.1 mmol/L, again, from baseline (Table 2). Changes in plasma HDL levels from baseline increased by 0.6 ± 0.1 mmol/L in OXM-104 mice, whereas plasma HDL levels decreased in OXM-101 mice by −1.1 ± 0.1 mmol/L (Table 2). Changes in plasma TG levels indicated a borderline-significant ($P = 0.060$) reduction for OXM-104 mice and a significant reduction in OXM-101 mice compared with vehicle (Table 2). Plasma TG levels decreased from baseline by −0.7 ± 0.3 mmol/L and −0.9 ± 0.2 mmol/L in OXM-104 and OXM-101 mice, respectively (Table 2).

Effects of Selective GLP-1/GCG Receptor Agonists on Liver Metabolism. The effects of OXM-104 and OXM-101 on liver metabolism were examined through the assessment of liver enzymes and liver histology (Fig. 4). Absolute liver weights of OXM-104 and OXM-101 mice were 3.2 ± 0.1 g and 1.8 ± 0.1 g, which corresponded to a 1.4-fold and 2.5-fold reduction in size compared with vehicle (Fig. 4A). Liver weights relative to body weight were approximately similar in size in OXM-104 and OXM-101 mice; both were significantly reduced from the vehicle, but no differences were observed between the two (Fig. 4B). Changes in liver enzymes, ALT, AST, and ALP from baseline were also investigated throughout the study (Fig. 4, C–E). ALT levels were significantly lowered when compared with vehicle. ALT levels in OXM-104 mice reduced ALT levels by 16.0% ± 11.4%, whereas OXM-101 mice decreased by 36.2% ± 4.8% (Fig. 4C). AST levels increased in all treatment groups, but progression was significantly lower in OXM-104 mice than in the vehicle and OXM-101 group (Fig. 4D). AST levels increased by 53.5% ± 16.9% and 149.0% ± 17.4% in OXM-104 and OXM-101 mice, respectively. ALP levels increased in all treatment groups from baseline, but only OXM-101 significantly differed from vehicle. ALP levels in OXM-104 and OXM-101 increased by 77.4% ± 27.7% and 245.8% ± 186.7%, respectively (Fig. 4E).

The basement type IV collagen formation marker PRO-C4 has previously been shown to reflect liver fibrosis in NASH rodents and was therefore measured at study end (Leeming et al., 2012; Boland et al., 2020). PRO-C4 levels were significantly reduced in OXM-104 and OXM-101 mice compared with vehicle (Fig. 4F). PRO-C4 levels decreased by 26.6% ± 5.3% in OXM-104 mice and 38.6% ± 7.7% in OXM-101 mice compared with vehicle. Histologic macro- and microsteatosis scores were significantly reduced in OXM-104 (only a nonsignificant tendency for microsteatosis lowering) and OXM-101 mice compared with vehicle (Fig. 4, G and I). No significant differences were observed in inflammation and fibrosis scores, but fibrosis scores showed a tendency for reduction in OXM-104 and OXM-101 mice compared with vehicle (Fig. 4, G and H).

Effects of Selective GLP-1/GCG Receptor Agonists on Glucose Control in Obese NASH Mice. Glucose control was examined in the obese NASH mice throughout the study. Repeated administration of OXM-104 and OXM-101 significantly lowered FBG levels compared with vehicle (Fig. 5A). OXM-104 and OXM-101 mice reduced FBG levels by 33.5% ± 3.9% and 34.4% ± 3.7% from baseline (Fig. 5B). Examination of body weight–independent effects of dual GLP-1/GCG receptor agonists on glucose control indicated a superiority of OXM-104 compared with OXM-101 (Fig. 5C). Plasma insulin levels measured at study end were mildly reduced in OXM-104 mice, whereas a significant reduction was observed
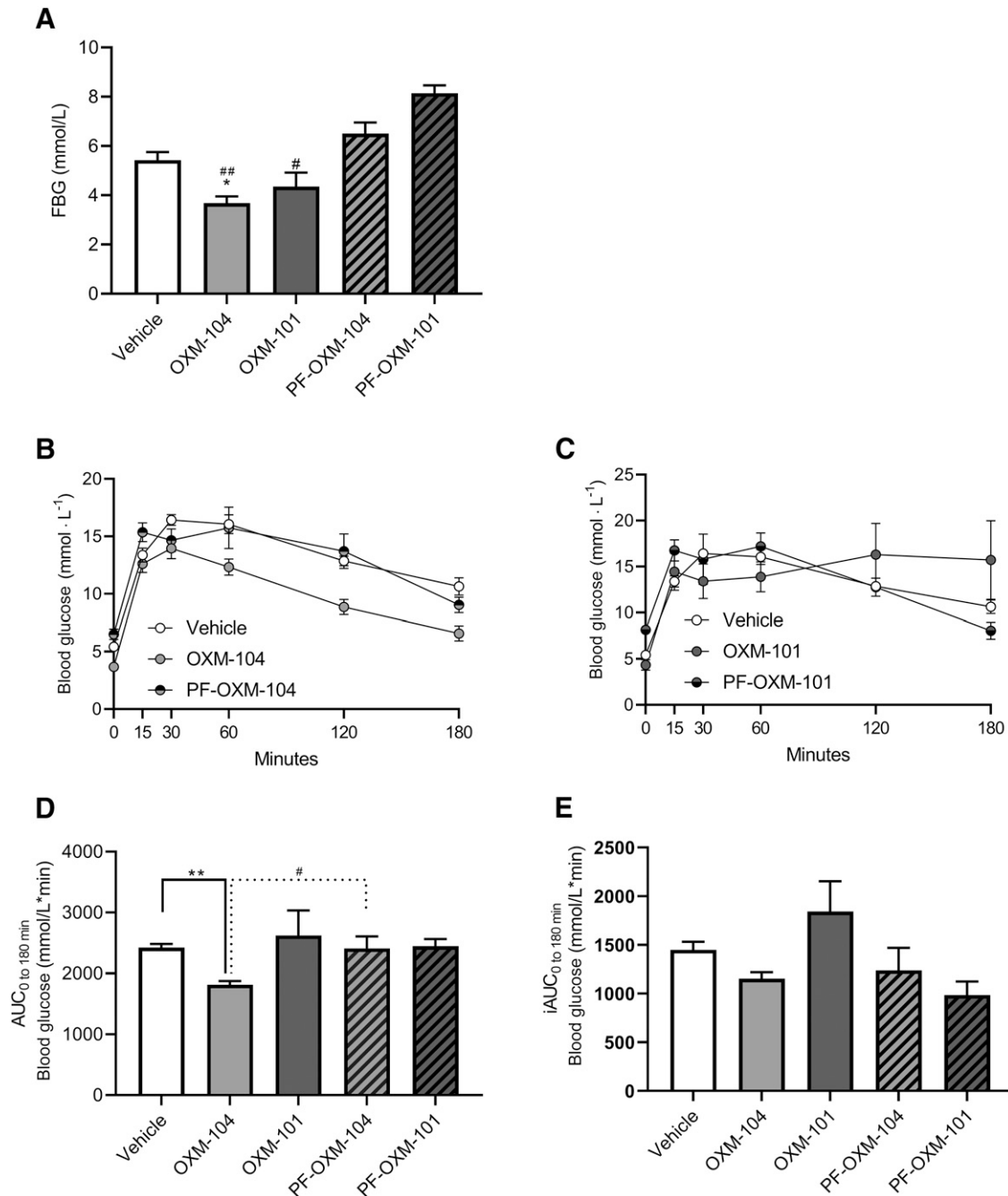
Fig. 2. Chronic administration of OXM-104 and OXM-101 significantly improves glucose tolerance in obese mice. (A) FBG levels at OGTT baseline. (B) Plasma glucose levels during end OGTT in mice dosed 24 hours before testing with vehicle ($n = 16$), OXM-104 ($n = 8$), and PF-OXM-104 ($n = 8$). (C) Plasma glucose levels during OGTT in mice dosed with vehicle ($n = 16$), OXM-101 ($n = 4$), and PF-OXM-101 ($n = 4$). (D) tAUC for blood glucose (mmol/L*min) in all treatment groups. (E) Incremental area under the curve (iAUC) for blood glucose (mmol/L*min) in all treatment groups. Statistical analysis between groups was evaluated by one-way ANOVA and Bonferroni's multiple comparison post hoc test, except for (A), which was analyzed by a Kruskal-Wallis test and Dunn's multiple comparison post hoc test. *$P < 0.05$; ** $P < 0.01$ compared with vehicle. #$P < 0.05$; ##$P < 0.01$ compared with the pair-fed groups. Data are mean ± S.E.M.

in OXM-101 mice compared with vehicle mice. (Fig. 5D). Plasma insulin levels in vehicle, OXM-104, and OXM-101 were 11.0 ± 0.8 ng/mL, 9.5 ± 1.2 ng/mL, and 1.5 ± 0.1 ng/mL, respectively (Fig. 5D).

Effects of Selective GLP-1/GCG Receptor Agonists on Glucose Tolerance in Obese NASH Mice. An OGTT was performed at study end to investigate effects on glucose tolerance. Chronic treatment effects were reflected in the baseline FBG levels (Fig. 6A). Repeated administration of OXM-

101 and OXM-104 affected glucose as indicated by differences in baseline FBG levels. At baseline, the mean FBG level was 7.5 ± 1.1 mmol/L in OXM-104–administered mice, 4.2 ± 0.9 mmol/L in OXM-101–administered mice, and 9.7 ± 1.6 mmol/L in vehicle mice. tAUC levels in OXM-104 and OXM-101 mice were significantly lowered compared with vehicle (Fig. 6B). The substantial reductions on body weight could drive the improved glucose tolerance observed in OXM-101 mice (Fig. 3A). Interestingly, incremental area-under-the-curve comparison
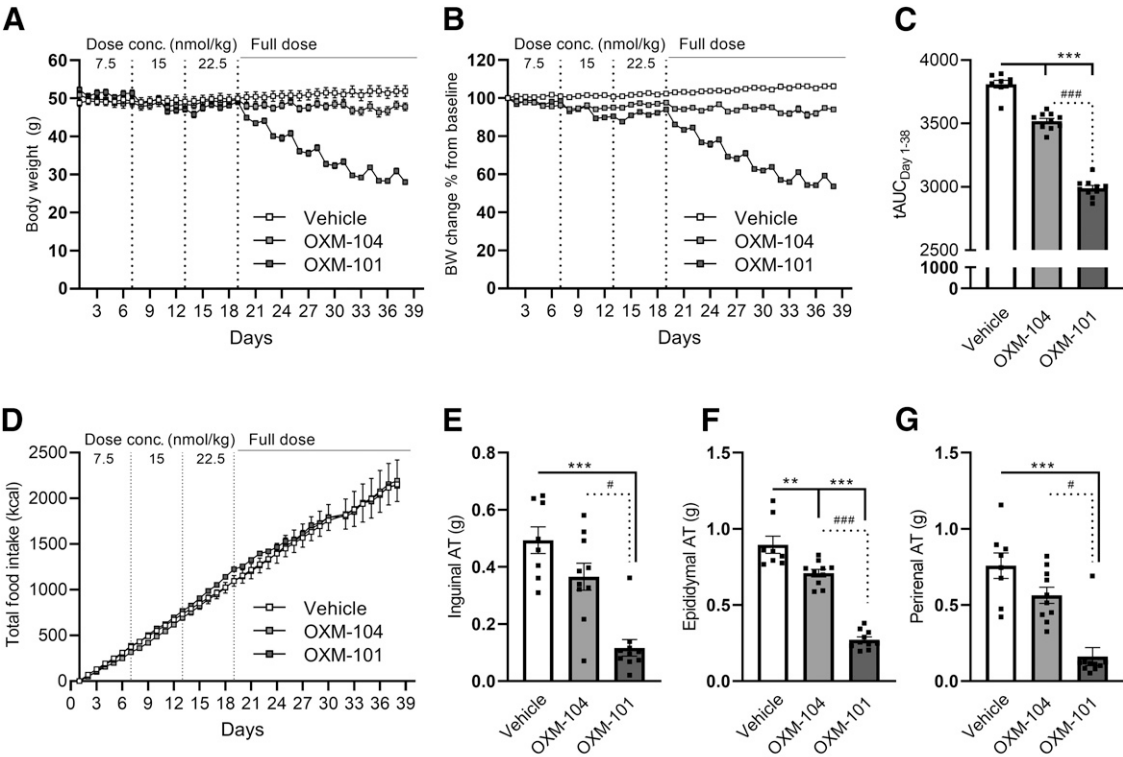
Fig. 3. Effects of OXM-104 and OXM-101 on body weight (bw), food intake, and adipose tissue depots in obese NASH mice. (A) Body weight and (B) body weight change (percentage of initial body weight) in obese NASH mice after 38 days of treatment with vehicle (n = 8), OXM-104 30 nmol/kg (n = 10), and OXM-101 30 nmol/kg (n = 10). (C) tAUC for body weight change (percentage of initial body weight) in all treatment groups. (D) Accumulated caloric intake expressed in kcal/4 mice. (E) Absolute inguinal adipose tissue weight. (F) Absolute epididymal adipose tissue weight. (G) Absolute perirenal adipose tissue weight. Dotted lines designate escalation timepoint. Statistical analysis between groups was evaluated by one-way ANOVA and Bonferroni's multiple comparison post hoc test, except for (E) and (G), which were evaluated by a Kruskal-Wallis test and Dunn's multiple comparison test. $**P < 0.01$; $***P < 0.001$ versus vehicle mice. $\#P < 0.05$; $\#\#\#P < 0.001$ versus OXM-104. Data are mean ± S.E.M.

between OXM-104 and OXM-101 showed no statistical difference but was significantly reduced compared with vehicle (Fig. 6C). This strongly suggests that the effects are derived from the weight improvements.

Discussion

Global health has been heavily burdened by the Western lifestyle for a long time, promoting metabolic dysfunctions such as obesity, type 2 diabetes, and NASH. Currently, no Food and Drug Administration–approved drugs for the treatment of NASH exist. Dual GLP-1/GCG receptor agonists have shown promise as antiobesogenic, antidiabetic, and anti-NASH treatments (Boland et al., 2020; Henderson et al., 2016; Elvert et

al., 2018). However, receptor selectivity in the context of NASH needs to be explored to maximize metabolic outcomes. The combination of direct liver action and insights on peptide selectivity can optimize outcome efficacies, thus reducing the gap between body weight–lowering effects of pharmacological interventions and surgery.

Dual GLP-1/GCG receptor agonists OXM-104 and OXM-101 were developed as a peptide program using evolutionary GCG and oxyntomodulin sequences. The peptide lengths of OXM-104 were chosen to mimic native oxyntomodulin and GCG for OXM-101. OXM-104 and OXM-101 were designed to provide approximal effects on glucose control, as shown in the in vitro screening. In contrast, we designed the GCG receptor component of OXM-104 and OXM-101 differently to provide shifted

TABLE 2
Lipid profiles of the vehicle, OXM-104 (30 nmol/kg), and OXM-101 (30 nmol/kg), presented as percentage of change from baseline
Levels of chol, LDL, HDL, and TG are presented as mean ± S.E.M. with the following annotations: $**P < 0.01$; $***P < 0.001$ versus vehicle (change). Statistical analysis between groups was evaluated by one-way ANOVA and Bonferroni's multiple comparison post hoc test.

|	Lipid Profile								
	Vehicle			OXM-104			OXM-101		
(mmol/L)	Baseline	Study End	Change %	Baseline	Study End	Change %	Baseline	Study End	Change %
Chol	5.1 ± 0.2	7.75 ± 0.39	21.9 ± 11.7	5.8 ± 0.2	5.59 ± 0.29	−4.5 ± 4.8***	6.1 ± 0.2	2.52 ± 0.13	−58.01 ± 2.0**
LDL	0.3 ± 0.02	0.76 ± 0.06	84.2 ± 45.2	0.4 ± 0.02	0.51 ± 0.05	33.1 ± 12.0**	0.4 ± 0.01	0.13 ± 0.01	−64.2 ± 4.9**
HDL	1.6 ± 0.1	3.16 ± 0.12	70.2 ± 33.9	1.7 ± 0.1	2.29 ± 0.09	36.5 ± 7.1***	1.7 ± 0.1	0.59 ± 0.06	−65.1 ± 2.2***
TG	1.8 ± 0.1	1.42 ± 0.03	−13.2 7.1	1.9 ± 0.1	1.15 ± 0.06	−36.2 ± 4.4 (P < 0.06)	1.9 ± 0.1	0.72 ± 0.04	−53.7 ± 3.3**
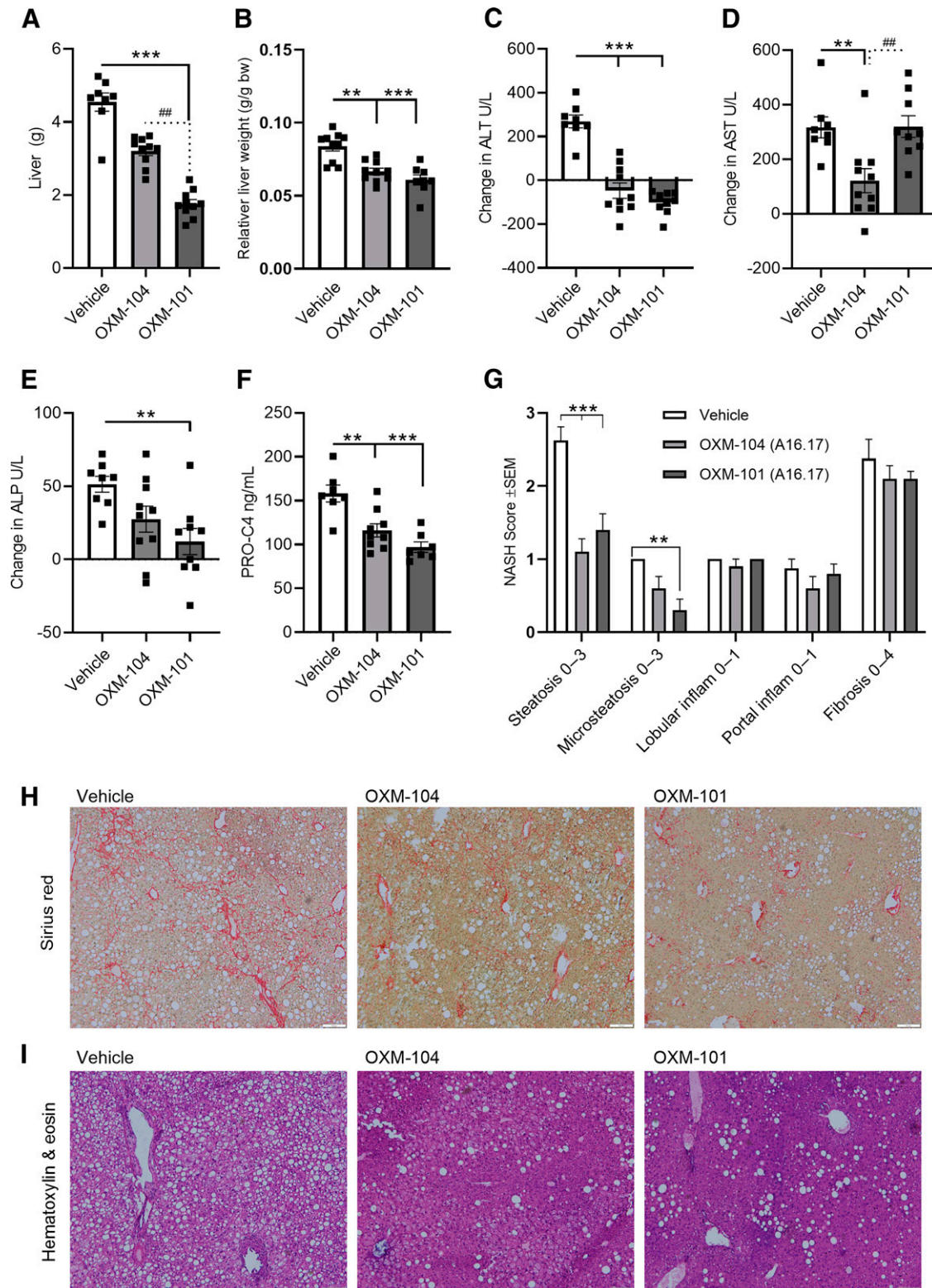
Fig. 4. Effects of OXM-104 and OXM-101 on lever metabolism in obese NASH following 38 days of administration with vehicle ($n = 8$), OXM-104 30 nmol/kg ($n = 10$), and OXM-101 30 nmol/kg ($n = 10$). (A) Absolute liver weight (g). (B) Relative liver weight. (C) Changes in liver enzymes from baseline are shown in (C) ALT (U/L), (D) AST (U/L), and (E) ALP (U/L). (F) PRO-C4 levels (ng/mL) at study end. (G) Steatosis, inflammation, and fibrosis scores. (H) Representative Sirius Red–stained liver sections. Scale bar, 100 μM. (I) Representative hematoxylin and eosin liver sections. Scale bar 100 μM. Statistical analysis between groups was evaluated by one-way ANOVA and Bonferroni's multiple comparison post hoc test, except for (A) and (B), which were analyzed by a Kruskal-Wallis test and Dunn's multiple comparison post hoc test. **$P < 0.01$; **$P < 0.01$ compared with vehicle. ##$P < 0.01$ compared with OXM-104. Data are mean ± S.E.M. bw, body weight.
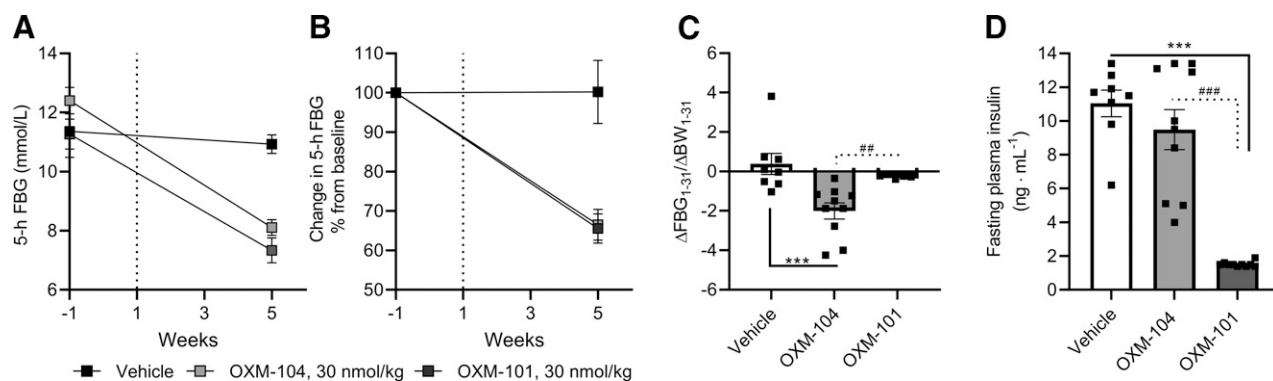
Fig. 5. Effects of OXM-104 and OXM-101 on glucose regulation in obese NASH mice. (A) Change in 5-hour FBG levels from baseline, shown as mmol/L, and (B) change in 5-hour FBG levels from baseline, shown as percentage of initial FBG. (C) Effects on glucose control beyond body weight (BW) shown as $\Delta FBG_{1-31}/\Delta BW_{1-31}$. (D) Plasma insulin levels (ng/mL) at study end. The dotted line shown in (A) and (B) designates the study start. Treatments are indicated as follows: vehicle ($n = 8$), OXM-104 30 nmol/kg ($n = 10$), and OXM-101 30 nmol/kg ($n = 10$). Statistical analysis between groups was evaluated by a Kruskal-Wallis test and Dunn's multiple comparison test in (C) and one-way ANOVA and Bonferroni's multiple comparison post hoc test for (D). ***$P < 0.001$ versus vehicle mice. ##$P < 0.01$ versus OXM-104; ###$P < 0.001$ versus OXM-104. Data are mean ± S.E.M.

effects on energy expenditure (Nair, 1987; Salem et al., 2016). OXM-104 was designed with an increased relative GLP-1 receptor activity (~44:1), whereas OXM-101 showed much greater GCG receptor potency (~10:1). Therapeutic candidates have been previously developed with both a balanced GLP-1/GCG receptor agonism [e.g., ALT-801 (Nestor et al., 2022; Nestor et al., 2021) and HM12525A (Jung et al., 2014)] and with an increased GLP-1 receptor activity [e.g., cotadutide SAR425899 and BI 456906 (Ambery et al., 2018b; Riber et al., 2018; Tillner et al., 2019)].

We observed that OXM-104 and OXM-101 induced reductions in body weight in obese and obese-NASH mice throughout both studies. Previously, body weight–lowering effects of dual GLP1/GCG receptor agonists have been reported (Ambery et al., 2018a; Tillner et al., 2019). Interestingly, OXM-101 significantly induced body weight reductions from OXM-104, possibly due to the increased relative GCG receptor activity. In line with the antiobesity effects observed using OXM-101, GCG receptor agonists have previously been shown to elicit marked reductions in body weight (Kim et al., 2019). Effects on body weight lowering beyond energy intake by OXM-101 were more significant than for OXM-104, possibly due to increased resting energy expenditure. Interestingly, infusions studies in humans have shown that GLP-1 does not affect

resting energy intake, whereas infusions of dual GLP-1/GCG and GCG alone increase resting energy expenditure (Scott et al., 2018).

We also observed reductions in inguinal and perirenal adipose tissue in both models, corresponding to a previous finding using balanced dual GLP-1/GCG receptor agonists (Day et al., 2009).

Glucose control and glucose tolerance during an OGTT were improved in OXM-104 mice in both obese and obese-NASH mice. Interestingly, SAR425899 and cotadutide, two dual GLP-1/GCG receptor agonists with increased relative GLP-1 receptor agonism (5:1), were found to improve glucose control in clinical trials (Ambery et al., 2018b; Tillner et al., 2019). The hyperglycemic risk associated with increased relative GCG receptor activity can have serious negative consequences if not correctly balanced. In obese mice, we found an impaired glucose tolerance using OXM-101. In contrast, OXM-101 in obese NASH mice showed improved glucose control and tolerance. This finding appeared to be driven by the considerable reduction in body weight, which improved insulin sensitivity, as indicated by the apparent insulin levels.

Similar to our findings, others used dual GLP-1/GCG receptor agonists with extreme receptor selectivity, reporting apparent body weight–lowering effects and suppression of caloric intake (Day et al., 2012). They reported that GCG selectivity
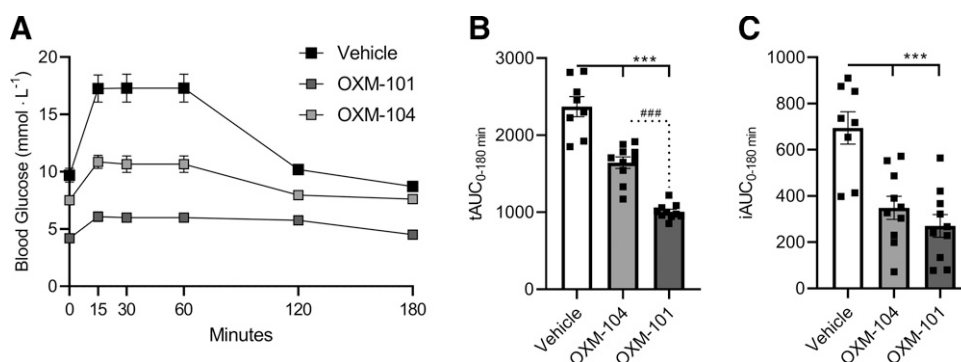

Fig. 6. Effects of OXM-104 and OXM-101 on glucose tolerance in obese NASH mice. (A) Plasma glucose levels during end OGTT in mice dosed 24 hours before testing with vehicle ($n = 8$), OXM-104 30 nmol/kg ($n = 10$), and OXM-101 30 nmol/kg ($n = 10$). (B) tAUC for blood glucose (mmol/L*min) in all treatment groups. Incremental area under the curve (iAUC) for blood glucose (mmol/L*min) in all treatment groups. Statistical analysis between groups was evaluated by one-way ANOVA and Bonferroni's multiple comparison post hoc test. ***$P < 0.001$ versus vehicle; #$P < 0.05$ versus OXM-104. Data are mean ± S.E.M.

had less impact on caloric intake and that adding 10% relative GLP-1 receptor agonism tripled the body weight–lowering effects and improved the hyperglycemic risk (Day et al., 2012). In obese NASH mice, body weight reductions during the dose-escalation period were similar between OXM-104 and OXM-101. Interestingly, treatment with OXM-101 elicited dramatic body weight reductions compared with OXM-104 at full dose. Our findings suggest the existence of a GCG receptor activity threshold, which, upon subthreshold doses, produces similar body weight–lowering effects regardless of selectivity. In contrast, suprathreshold doses may result in additional activation of direct GCG receptor-mediated anorexic and lipolytic pathways. In line with this finding, GCG effects at low doses ($\sim$14 nmol/kg) have been shown to induce hyperphagia, whereas at high doses ($\sim$115 nmol/kg) have been shown to reduce food intake in rats (Geary and Smith, 1983; Hell and Timo-Iaria, 1985).

Dual GLP-1/GCG receptor agonists show promise as a potential NASH treatment due to the direct liver action. In obese NASH mice, OXM-104 and OXM-101 reduced PRO-C4 levels to a similar extent compared with vehicle. Collagen formation marker PRO-C4 recognizes the 7S domain of collagen type IV (P4NP7S), which was previously shown to be associated with liver fibrosis (Leeming et al., 2012). Furthermore, the effects of OXM-104 and OXM-101 on liver function showed reduced ALT levels compared with vehicle. Similarly, 6 weeks of cotadutide treatment in ob/ob mice reduced levels of P4 NP7S and ALT (Boland et al., 2020). AST levels in OXM-104 mice decreased compared with the vehicle, whereas OXM-101 mice maintained similar AST levels as the vehicle. In contrast, cotadutide treatment in ob/ob mice increased AST levels compared with vehicle (Boland et al., 2020). Additionally, a tendency for reduction in ALP levels was observed in OXM-104 mice compared with vehicle. OXM-101 mice reduced ALP levels compared with control. In line with this finding, ALP levels were reduced in liraglutide-treated mice with acute liver injury (Milani et al., 2019). Overall, improved NAFLD activity scores were observed using both OXM-104 and OXM-101.

The improved liver fat reductions have been suggested to be due to the direct impact of GCG agonism to inhibit lipogenesis while enhancing mitochondrial turnover and oxidative capacity (Boland et al., 2020). This finding underlines the importance of GCG agonism and its potential as a future anti-NASH therapy. Therefore, we suggest that future dual GLP-1/GCG receptor agonists can be developed in a more personalized manner. Lean subjects with NASH can potentially be introduced to therapy with increased relative GLP-1 receptor agonism. In contrast, morbidly obese NASH subjects could receive treatment with increased relative GCG receptor activity to induce a more significant reduction in body weight. This reasoning requires the development of selective GCG receptor-agonists with improved glucose control to test the hypothesis.

Based on our findings, we confirm the potential of dual GLP-1/GCG receptor agonists as a treatment of NASH as both peptides improved liver health and steatosis. The most crucial consideration is the hyperglycemic risk associated with increased GCG receptor activity. The safest developmental choice is to initiate a peptide program focused on peptides with increased relative GLP-1 receptor agonism. Moreover, increased body weight lowering is favorable for metabolism. With the marked increase in obesity prevalence, we suggest that future peptide designs should be arranged with a slightly increased GCG receptor

activity without disrupting glucose control to reduce the gap between surgery versus pharmacological treatment.

Conclusion

The current study indicates that an agonist with increased relative GLP-1 receptor activity is favored over an agonist with increased relative GCG receptor activity due to lower hyperglycemic risk. Furthermore, dual GLP-1/GCG receptor agonist as potential therapies for NASH is kept intact as both peptides provide healthy liver and lipid profiles.

Limitations. This study included pair-feeding groups as a surrogate marker for energy expenditure. In future studies, metabolic cages should be used to directly measure energy expenditure. Furthermore, diet compositions can be further enhanced to provide a more translational milieu. Future studies should have a natural reference, such as oxyntomodulin, as it may indicate what an optimal receptor selectivity is to obtain maximized metabolic effects.

The data supporting this manuscript's findings are available from the corresponding author upon reasonable request.

Authorship Contributions

Participated in research design: Kayed, Henriksen.
Conducted experiments: Kayed, Melander, Khan.
Performed data analysis: Kayed, Melander, Andreassen, Henriksen.
Wrote or contributes to the writing of the manuscript: Kayed, Melander, Andreassen, Karsdal, Henriksen.

References

Ambery P, Parker VE, Stumvoll M, Posch MG, Heise T, Plum-Moerschel L, Tsai L-F, Robertson D, Jain M, Petrone M, et al. (2018a) MEDI0382, a GLP-1 and glucagon receptor dual agonist, in obese or overweight patients with type 2 diabetes: a randomised, controlled, double-blind, ascending dose and phase 2a study. *Lancet* **391**:2607–2618.

Ambery PD, Klammt S, Posch MG, Petrone M, Pu W, Rondinone C, Jermutus L, and Hirshberg B (2018b) MEDI0382, a GLP-1/glucagon receptor dual agonist, meets safety and tolerability endpoints in a single-dose, healthy-subject, randomized, Phase 1 study. *Br J Clin Pharmacol* **84**:2325–2335.

Armstrong MJ, Hull D, Guo K, Barton D, Hazlehurst JM, Gathercole LL, Nasiri M, Yu J, Gough SC, Newsome PN, et al. (2016) Glucagon-like peptide 1 decreases lipotoxicity in non-alcoholic steatohepatitis. *J Hepatol* **64**:399–408.

Boland ML, Laker RC, Mather K, Nawrocki A, Oldham S, Boland BB, Lewis H, Conway J, Naylor J, Guionaud S, et al. (2020) Resolution of NASH and hepatic fibrosis by the GLP-1R/GcgR dual-agonist Cotadutide via modulating mitochondrial function and lipogenesis. *Nat Metab* **2**:413–431.

Day JW, Gelfanov V, Smiley D, Carrington PE, Eiermann G, Chicchi G, Erion MD, Gidda J, Thornberry NA, Tschöp MH, et al. (2012) Optimization of co-agonism at GLP-1 and glucagon receptors to safely maximize weight reduction in DIO-rodents. *Biopolymers* **98**:443–450.

Day JW, Ottaway N, Patterson JT, Gelfanov V, Smiley D, Gidda J, Findeisen H, Bruemmer D, Drucker DJ, Chaudhary N, et al. (2009) A new glucagon and GLP-1 co-agonist eliminates obesity in rodents. *Nat Chem Biol* **5**:749–757.

Elvert R, Herling AW, Bossart M, Weiss T, Zhang B, Wenski P, Wandschneider J, Kleutsch S, Butty U, Kannt A, et al. (2018) Running on mixed fuel-dual agonistic approach of GLP-1 and GCG receptors leads to beneficial impact on body weight and blood glucose control: A comparative study between mice and non-human primates. *Diabetes Obes Metab* **20**:1836–1851.

Geary N and Smith GP (1983) Selective hepatic vagotomy blocks pancreatic glucagon's satiety effect. *Physiol Behav* **31**:391–394.

Graham GV, Conlon JM, Abdel-Wahab YH, and Flatt PR (2018) Glucagon-related peptides from phylogenetically ancient fish reveal new approaches to the development of dual GCGR and GLP1R agonists for type 2 diabetes therapy. *Peptides* **110**:19–29 Elsevier.

Gydesen S, Andreassen KV, Hjuler ST, Christensen JM, Karsdal MA, and Henriksen K (2016) KBP-088, a novel DACRA with prolonged receptor activation, is superior to davalintide in terms of efficacy on body weight. *Am J Physiol Endocrinol Metab* **310**:E821–E827.

Hell NS and Timo-Iaria C (1985) Increase of food intake induced by glucagon in the rat. *Physiol Behav* **34**:39–44.

Henderson SJ, Konkar A, Hornigold DC, Trevaskis JL, Jackson R, Fritsch Fredin M, Jansson-Löfmark R, Naylor J, Rossi A, Bednarek MA, et al. (2016) Robust anti-obesity and metabolic effects of a dual GLP-1/glucagon receptor peptide agonist in rodents and non-human primates. *Diabetes Obes Metab* **18**:1176–1190.

Henriksen K, Bay-Jensen AC, Christiansen C, and Karsdal MA (2010) Oral salmon calcitonin–pharmacology in osteoporosis. *Expert Opin Biol Ther* **10**:1617–1629.

Holst JJ (2007) The physiology of glucagon-like peptide 1. *Physiol Rev* **87**:1409–1439.

Jung SY, Park YJ, Kim JK, Lee JS, Lee YM, Kim YH, Kang JH, Trautmann M, Hompesch M, and Kwon SC (2014) Lipolytic and insulinotropic effects of HM12525A, a novel long-acting GLP-1/glucagon dual agonist. Presented at EASH Meeting, 2014. Availible at: https://www.easd.org/media-centre/home.html#!resources/lipolytic-and-insulinotropic-effects-of-hm12525a-a-novel-long-acting-glp-1-glucagon-dual-agonist–2 (Accessed 91 dec 2022).

Katri A, Dąbrowska A, Löfvall H, Ding M, Karsdal MA, Andreassen KV, Thudium CS, and Henriksen K (2019) Combining naproxen and a dual amylin and calcitonin receptor agonist improves pain and structural outcomes in the collagen-induced arthritis rat model. *Arthritis Res Ther* **21**:68.

Kim JK., Kim J., Lee SM, Lee J, Lee SH, and Choi IY (2019) 991-P: Potential of a Novel Long-Acting Glucagon Analog, HM15136, for the Treatment of Obesity. *Diabetes* **68** (Suppl 1):991-P.

Leeming DJ, Nielsen MJ, Dai Y, Veidal SS, Vassiliadis E, Zhang C, He Y, Vainer B, Zheng Q, and Karsdal MA (2012) Enzyme-linked immunosorbent serum assay specific for the 7S domain of Collagen Type IV (P4NP 7S): A marker related to the extracellular matrix remodeling during liver fibrogenesis. *Hepatol Res* **42**:482–493.

Milani L, Galindo CM, Turin de Oliveira NM, Corso CR, Adami ER, Stipp MC, Beltrame OC, and Acco A (2019) The GLP-1 analog liraglutide attenuates acute liver injury in mice. *Ann Hepatol* **18**:918–928.

Müller TD, Finan B, Clemmensen C, Dimarchi RD, and Tschöp MH (2017) The New Biology and Pharmacology of Glucagon. *Physiol Rev* **97**:721–766.

Nair KS (1987) Hyperglucagonemia increases resting metabolic rate in man during insulin deficiency. *J Clin Endocrinol Metab* **64**:896–901.

Nestor JJ, Zhang X, Jaw-Tsai S, Parkes DG, and Becker CK (2021) Design and characterization of a surfactant-conjugated, long-acting, balanced GLP -1/glucagon receptor dual agonist. *Peptide Science* **113**.

Nestor JJ, Parkes D, Feigh M, Suschak JJ, and Harris MS (2022) Effects of ALT-801, a GLP-1 and glucagon receptor dual agonist, in a translational mouse model of non-alcoholic steatohepatitis. *Sci Rep* **12**.

O'Harte FPM, Ng MT, Lynch AM, Conlon JM, and Flatt PR (2016) Dogfish glucagon analogues counter hyperglycaemia and enhance both insulin secretion and action in diet-induced obese diabetic mice. *Diabetes Obes Metab* **18**:1013–1024.

Riber D, Tolborg JL, Hamprecht DW, Thomas, L (2018) Acylated Glucagon Analogue, US Patent 15/566,338. 2018.

Salem V, Izzi-Engbeaya C, Coello C, Thomas DB, Chambers ES, Comninos AN, Buckley A, Win Z, Al-Nahhas A, Rabiner EA, et al. (2016) Glucagon increases energy expenditure independently of brown adipose tissue activation in humans. *Diabetes Obes Metab* **18**:72–81.

Newsome PN, Buchholtz K, Cusi K, Linder M, Okanoue T, Ratziu V, Sanyal AJ, Sejling AS, and Harrison SA (2021) A Placebo-Controlled Trial of Subcutaneous Semaglutide in Nonalcoholic Steatohepatitis. *N Engl J Med* **384**:1113–1124.

Scott R, Minnion J, Tan T, and Bloom SR (2018) Oxyntomodulin analogue increases energy expenditure via the glucagon receptor. *Peptides* **104**:70–77.

Sexton PM, Findlay DM, and Martin TJ (1999) Calcitonin. *Curr Med Chem* **6**:1067–1093.

Tillner J, Posch MG, Wagner F, Teichert L, Hijazi Y, Einig C, Keil S, Haack T, Wagner M, Bossart M, et al. (2019) A novel dual glucagon-like peptide and glucagon receptor agonist SAR425899: Results of randomized, placebo-controlled first-in-human and first-in-patient trials. *Diabetes Obes Metab* **21**:120–128.

Younossi Z, Anstee QM, Marietti M, Hardy T, Henry L, Eslam M, George J, and Bugianesi E (2018) Global burden of NAFLD and NASH: trends, predictions, risk factors and prevention. *Nat Rev Gastroenterol Hepatol* **15**:11–20.

Address correspondence to: Simone Anna Melander, Nordic Bioscience A/S, Herlev Hovedgade 207, DK-2730, Herlev, Denmark. E-mail: sme@nordicbio.com

Article Title

The effects of dual GLP-1/GCG receptor agonists with different receptor selectivity in mouse models of obesity and NASH

Ashref Kayed, Simone Anna Melander, Suheb Khan, Kim Vietz Andreassen, Morten Asser Karsdal, Kim Henriksen

Nordic Bioscience Biomarkers and Research, Department of Endocrinology, Herlev Hovedgade 207, Herlev, Denmark
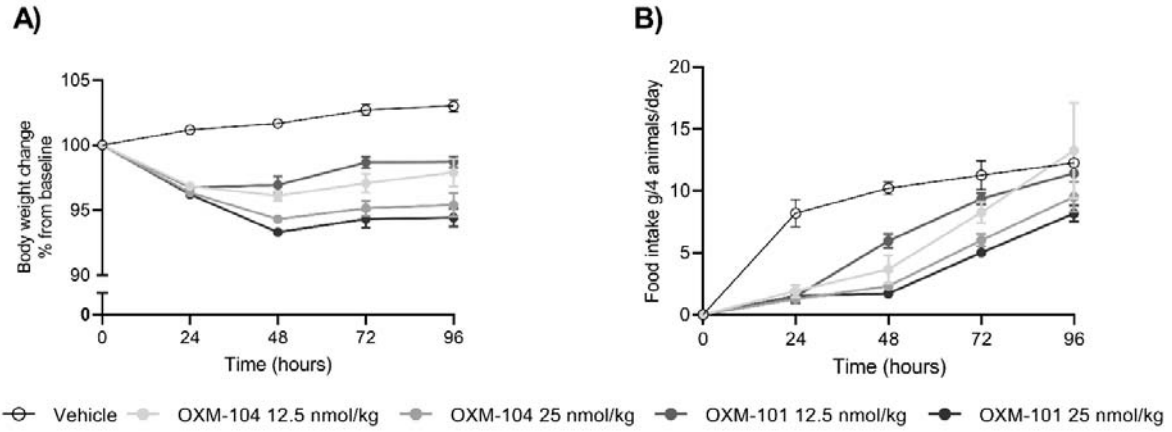
Supplementary Figures

Figure 1S. Acute *in vivo* potency testing of OXM-104 and OXM-101. Mice received a single subcutaneous injection of OXM-104 12.5 nmol/kg (n=8), OXM-104 25 nmol/kg (n=8), OXM-101 12.5 nmol/kg (n=8) and OXM-101 25 nmol/kg (n=8). A) Body weight changes (% of initial body weight. B) Daily food intake during the acute test (g/4 animals). Data are mean ± SEM.
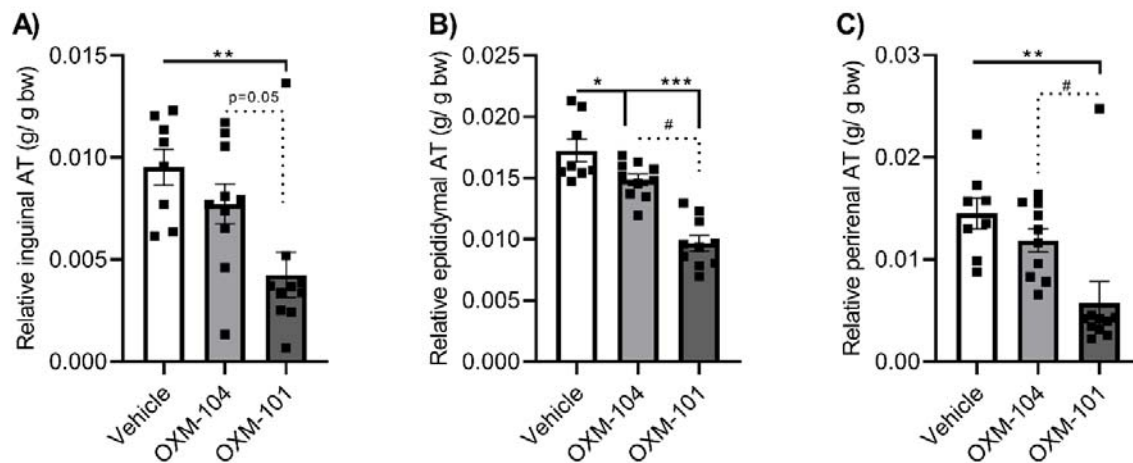
Figure S2. Adipose tissue weights relative to body weight in obese NASH mice treated with OXM-104 and OXM-101. Relative weights of A) Inguinal adipose tissue, B) epididymal adipose tissue, and C) perirenal adipose tissue. *$p<0.05$ ** $p<0.01$ *** $p<0.001$ vs Vehicle mice. # $p<0.05$ ## $p<0.01$ vs. OXM-104. Statistical analysis between groups was evaluated by one-way ANOVA and Bonferroni's multiple comparison post-hoc test except for A and c), evaluated by a Kruskal Wallis test, and Dunn's multiple comparison test. Data are mean ± SEM.